iTransformer Network Based Approach for Accurate Remaining Useful Life Prediction in Lithium-Ion Batteries

Anurag Jha
McMaster Automotive Resource Centre (MARC)
McMaster University
Hamilton, ON L8P0A6, Canada
jhaa14@mcmaster.ca

Oorja Dorkar
McMaster Automotive Resource Centre (MARC)
McMaster University
Hamilton, ON L8P0A6, Canada
dorkaro@mcmaster.ca

Atriya Biswas
McMaster Automotive Resource Centre (MARC)
McMaster University
Hamilton, ON L8P0A6, Canada
biswaa4@mcmaster.ca

Ali Emadi
McMaster Automotive Resource Centre (MARC)
McMaster University
Hamilton, ON L8P0A6, Canada
emadi@mcmaster.ca

2024 IEEE Transportation Electrification Conference and Expo (ITEC) | 979-8-3503-1766-4/24/$31.00 ©2024 IEEE | DOI: 10.1109/ITEC60657.2024.10598898

***Abstract*— Electric vehicles (EVs) are paving the way toward a sustainable future by reducing carbon footprints and gaining widespread global acceptance; predicting the EV battery's remaining useful life (RUL) is crucial. As the Li-ion batteries degrade and lose lithium and active material, managing the battery's state of health and charge is necessary to prevent it from reaching its End of Life (EOL). This paper explores a unique application of the iTransformer neural network for RUL prediction using multi-channel charging profiles. This implementation adopts multivariate forecasting, taking advantage of mapping the high-dimensional features to low-dimensional spaces by using the inverted self-attention mechanism to learn the distinctions and interactions between the time-series data. The iTransformer is applied to two popular open-source Li-ion battery datasets: NASA and CALCE. This technique is compared against existing techniques like the Long Short-Term Memory (LSTM) and Vanilla Transformer. The proposed iTransformer improves the root mean square error (RMSE) by 44.62% and 29% for the NASA and CALCE datasets, respectively, compared to the next best-evaluated methods.**

Keywords— Electric Vehicles, iTransformer, Lithium-ion batteries, Remaining Useful Life, State of Health

I. INTRODUCTION

As the transportation industry doubles down on efforts to achieve reduced emissions, EVs emerge as a cleaner, sustainable solution for transportation. To promote the wider adoption of EVs, several challenges must be addressed. Since the batteries are subjected to nonlinear degradation, it is crucial to predict their remaining useful life (RUL), which is a key marker of its End of Life (EOL) [1]. External factors, including repeated charging/discharging cycles, temperature, and charge/discharge rates, along with internal factors such as electrode material aging, electrolyte consumption, and SEI film formation/destruction, cause the aging of Li-ion batteries [2]. As the battery's capacity declines and its internal impedance rises, RUL estimation ensures that the batteries are operating in reliable conditions [3]. The battery aging trajectory is based on its usage history and helps in understanding future degradation by estimating the number of cycles remaining until the failure threshold.

RUL estimations are broadly classified into adaptive filter techniques, stochastic techniques, and data-driven techniques [4]. Physics-based approaches model the physiochemical phenomena and offer in-depth insights on degradation suited for nonlinear systems. Yu et al. incorporated a novel battery health criterion in a state-space model using Bayesian inference probability to predict RUL [5]. Su et al. introduced the interaction of multi-model particle filter to integrate multiple LIB capacity models [6]. However, its performance is dependent on the parameter distributions prior to the Bayesian updating process [7].

Deep learning has demonstrated remarkable success in tackling the nonlinear aspects of battery capacity and deterioration trends. Zhang et al. used a Recurrent Neural Network (RNN) to identify the hidden dependencies in battery capacity degradation, achieving better RUL prediction outcomes [8]. Jungsoo et al. discussed the design of Multi-Layer Perceptron (MLP) on discrete data with high accuracy [9]. Chinomona et al. implemented a Long Short-Term Memory (LSTM) network for RUL prediction using partial cycle data [10]. Song et al. proposed an RNN-Gate Recurrent Unit (GRU) for higher computational complexity [11]. While these methods are suitable for modeling sequential data, they struggle to handle long-range dependencies. Their effectiveness is also impacted by the battery's dynamic and nonlinear characteristics.

Transformers are recognized for their proficiency in text encoding and computer vision (CV) using the attention mechanism to learn long-term dependencies [12]. Given the advantages of Transformers in handling large sequences, this paper proposes the application of the 'iTransformer', which applies the attention and the feed-forward network (FFN) on the inverted dimensions to learn nonlinear representations for time-series forecasting [13]. In this paper, 'iTransformer' is being applied for the first time for RUL prediction for Li-ion batteries.

It is compared against the established benchmark LSTM and the original Vanilla Transformer.

II. Transformer Network for Time-Series Forecasting

A. Problem Statement

RUL forecast needs to be done accurately and on time to give a battery owner adequate notice of any possible hazards [14]. A crucial marker of battery aging is its State of Health (SOH), which captures the state of the battery as it undergoes charging-discharging cycles. The SOH can be calculated by the following equation:

$$SOH\ (t) = \frac{C_t}{C_0}\ x\ 100\% \qquad (1)$$

where C_0 , C_t denote the nominal capacity and measured capacity at time t, respectively. The battery's capacity reduces with an increase in charge/discharge cycles. The battery is said to reach its End of Life (EOL) when its capacity falls to 70–80% of the initial capacity [15].

B. iTransformer for RUL Prediction

Transformers have emerged at the forefront of deep learning methods in a wide number of fields, including Natural Language Processing (NLP), and are capable of processing sequential data, extracting relevant features, and modeling complex relationships with higher accuracy [12]. Battery degradation is a function of several features, such as voltage, temperature, current, internal resistance, and capacity. Many of these features are independent measurements that depend on the aging cycles. Therefore, RUL prediction can be posed as a time series problem with multiple variates.

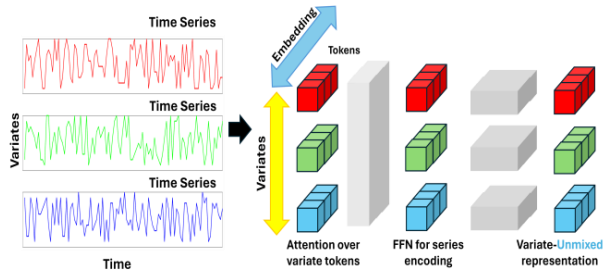

Fig. 1. The iTransformer methodology [13]

In the original Vanilla Transformer, the variates at a given time step are embedded into a single token, which suppresses the multivariate correlations. To alleviate this issue, the iTransformer was proposed, which takes an inverted view of the time series while preserving the original transformer architecture. The method embeds independent time series into separate variate tokens and employs self-attention to capture multivariate correlations [13]. The iTransformer consists of stacked blocks containing multivariate attention modules, layer normalization modules, and FFN. It encodes time series data through FFN and decodes future series representations. Individual variate representations are subjected to layer normalization, which handles non-stationary issues well and minimizes measurement inconsistencies. The self-attention module assesses correlations within each variate series, providing a clear approach to multivariate forecasting, as depicted in Fig.1.

III. Experimental Datasets

In this work, two frequently used open-source Li-ion battery datasets are used for RUL prediction by iTransformer modeling: NASA (5,6,7 & 18) and CALCE (CS2-35, 36, 37 & 38) datasets [16], [17]. The NASA dataset has a collection of data on four battery packs: B0005, B0006, B0007, and B0018.

The group of four lithium-ion batteries underwent three operational cycles: (i) charging, (ii) discharging, and (iii) impedance. All data measurements were conducted under standard room temperature conditions. Charging followed a constant current (CC) mode at 1.5A until the battery voltage reached 4.2V, transitioning thereafter to constant voltage (CV) mode until the charge current decreased to 20mA. Discharge followed a CC mode at 2A until the battery voltage dropped to 2.7V, 2.5V, 2.2V, and 2.5V for batteries 5, 6, 7, and 18, respectively [18]. The aging is accelerated by the continuous charging and discharging cycles of the battery. The impedance measurement gives information about the increased internal impedance of the battery due to aging. The experiments concluded upon meeting the end-of-life (EOL) criteria, defined as a 30% decrease in rated capacity from 2Ah to 1.4Ah. The capacity degradation curves for this dataset in shown in Fig. 2.

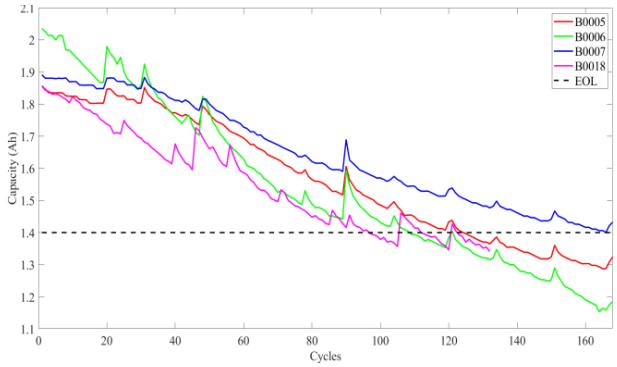

Fig. 2. Battery capacity degradation: NASA dataset [16]

The CALCE dataset for the given batteries, CS2-35, CS2-36, CS2-37, and CS2-38, is $LiCoO_2$ cathode type, and the capacity of the batteries under consideration is 1.1Ah. The cells were charged using the same profile, which was a conventional protocol of constant voltage/current at a constant rate of 1C until the voltage reached 4.2V. Following this, the voltage was kept constant at 4.2V until the charge current dropped under 0.05A. The cut-off limit for voltage during discharging was set at 2.7V [19]. As this dataset has information regarding capacity degradation and impedance increment, it is very useful for RUL

and SOH prediction. The capacity degradation curve for this dataset is shown in Fig. 3.

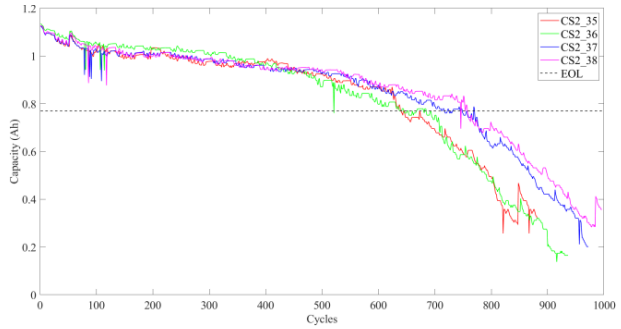

Fig. 3. Battery capacity degradation: CALCE dataset [17]

IV. METHODOLOGY

A. RUL Prediction Approach

a) Single Channel time series: This approach utilizes the battery's past capacity data C_K to generate data sequences with a time window of length L. The window length denotes the number of previous cycles the model can access to predict the future capacity. At any given cycle K, the past L cycles are used to generate the sequence $\{C_{K-L},\ldots\ldots C_K\}$, which is then used to predict C_{K+1}. This predicted capacity is combined with the original data to generate the next sequence $\{C_{K-L+1},\ldots\ldots C_{K+1}\}$ to predict the capacity C_{K+2}. The method is repeated recursively until all the sequences are generated.

b) Multi-channel time series: Along with the battery's capacity data, the voltage, current, and temperature (NASA)/ resistance (CALCE) charging profiles can also be used to characterize battery degradation. In the NASA battery dataset, the aged cell reaches its peak voltage of 4.2V earlier and its current drops earlier compared to a fresh cell. Additionally, the peak battery temperature is attained faster in an aged cell. Thus, it is evident that the SOH influences these charging profiles and, therefore, can be used as input features to our model. The large number of data points of these features must be down-sampled for better training of our neural network. After uniform downsampling, the data points for each input feature are concatenated into a feature vector.

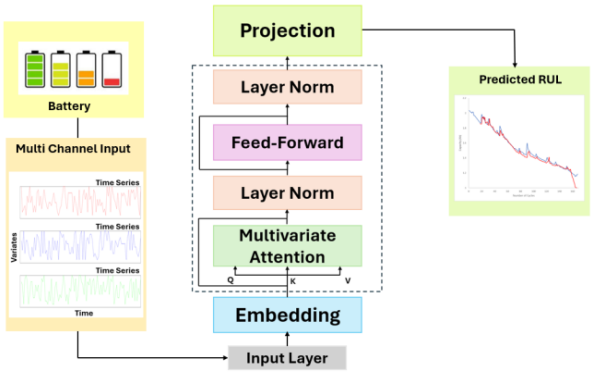

Fig. 4. The iTransformer architecture for RUL prediction

B. Data Preprocessing & Training

Before proceeding to the prediction model, the charging profiles are first cleaned to remove abnormal data. For efficient learning of the network, 10 points are uniformly sampled and averaged over the sampling interval for each of the temperature, current, and voltage profiles [20]. As the input features have different scales, normalization is performed to mitigate any effects of data distribution on the model training. Min-max normalization is utilized as per the following equation [21]:

$$X_K^S = \frac{x_K^S - \min(\boldsymbol{x})}{\max(\boldsymbol{x}) - \min(\boldsymbol{x})} \quad S \in \{1, 2, \ldots., S-1, S\} \qquad (2)$$

where $\boldsymbol{x}$ is the set of charging cycles $\{x_K^S\}$. Since there are only four battery records present in these datasets, a 3-fold cross-validation is performed. For each battery selected in the testing set, two batteries are selected in the training set and one in the validation set. This procedure is applied thrice for all possible validation sets. The entire process is executed for the four batteries separately, and the average of the evaluation metrics is reported.

C. iTransformer Architecture

The iTransformer is based on the encoder-only structure of the Vanilla Transformer consisting of the Embedding, Multivariate Attention, Feed-forward Network, and Projection blocks as shown in Fig. 4. Given a time series $X = \{x_1,\ldots,x_T\} \in R^{T \times N}$ with T time steps and N features, X(:,n) represents the entire observation set for each feature n.

a) Embedding: The input variates are mapped to generate embedded tokens of dimension D. Positional encoding is used to inject information about the relative position of the sequences. The embedded token of dimension D for feature n is given by:

$$\boldsymbol{h}_n^0 = Embedding\left(X_{:,n}\right) \qquad (3)$$

b) Multivariate Attention: This layer captures the dependencies between features by applying the self-attention mechanism on each variate time series. Given the representation of each time series $H^l = \{\mathbf{h}_1,\ldots,\mathbf{h}_N\}$ at the l-th layer, the queries, keys, and values Q, K, V are generated through linear projections.

$$Attention\ (\boldsymbol{Q}, \boldsymbol{K}, \boldsymbol{V}) = softmax\left(\frac{\boldsymbol{Q}\boldsymbol{K}^T}{\sqrt{d_k}}\right)\boldsymbol{V} \qquad (4)$$

$$head_i = Attention\left(\boldsymbol{H}^{l-1}\boldsymbol{W}_Q^l, \boldsymbol{H}^{l-1}\boldsymbol{W}_K^l, \boldsymbol{H}^{l-1}\boldsymbol{W}_V^l\right) \qquad (5)$$

$$MultiHead\ (\boldsymbol{H}^{l-1}) = [head_1; \ldots; head_h]\boldsymbol{W}^O \qquad (6)$$

where $\boldsymbol{W}_Q^l$, $\boldsymbol{W}_Q^l$, and $\boldsymbol{W}_Q^l \in R^{D \times d_k}$ are projection weights.

c) Feed-forward Network (FFN): The series representation of each variate token is encoded by the network. Nonlinear dense layers are used to extract the complex

relationships of the input series. Every token is fed to the FFN identically and separately.

$$\boldsymbol{H}^{l} = FFN\big(MultiHead(\boldsymbol{H}^{l-1})\big) \tag{7}$$

d) Projection: A fully connected layer maps the output from the feed-forward network to get the predicted capacity at the next time step.

$$\hat{Y}_{:,n} = Projection(\boldsymbol{h}_n^L) \tag{8}$$

D. Model Selection

The proposed iTransformer model is compared to the Vanilla Transformer and the LSTM implementations. Both the single-channel and multi-channel approaches are investigated. The key parameters for the models are the lookback window size (WS), learning rate (LR), and size of hidden dimensions (HD) in the selected model. These parameters are tuned to minimize the validation error using the grid-search method. All the models are built using the Pytorch framework in Python with an Intel i9 CPU and 32 GB memory. The ReLU function is used for activation, and the Adam optimizer minimizes the losses.

E. Evaluation Metrics

In this paper, three evaluation metrics, namely, mean absolute error (MAE), root mean squared error (RMSE), and relative error (RE), are used to gauge model performance in RUL prediction. These metrics are selected due to their proven evaluation qualities for time series forecasting problems.

$$RMSE = \sqrt{\frac{1}{N}\sum_{n=1}^{N}\left(Y_n - \widehat{Y_n}\right)^2} \tag{9}$$

$$MAE = \frac{1}{N}\sum_{n=1}^{N}\left|Y_n - \widehat{Y_n}\right| \tag{10}$$

$$RE = \left|\frac{RUL_{pred} - RUL_{true}}{RUL_{true}}\right| \tag{11}$$

V. Result Discussion

In this study, we examine five distinct methods for predicting Remaining Useful Life (RUL). These methods include the Single Channel (SC) approach, utilizing only capacity sequences as input (SC-LSTM and SC-Transformer), and the Multi-Channel (MC) approach incorporating capacity, voltage, current, and temperature (NASA) / resistance (CALCE) as input (MC-LSTM, MC-Transformer, and MC-iTransformer).

A. Parameter Tuning

For accurate performance of the implemented models, it is necessary to get the optimal set of parameters as outlined in the previous section. For the iTransformer, the search space for the different parameters is: Lookback Window Size ∈ [16, 32, 64, 128]; size of Hidden Dimensions ∈ [16, 32, 64, 128]; Learning Rate ∈ [10^{-3}, 5 x 10^{-3}, 10^{-2}, 5 x 10^{-2}, 2 x 10^{-1}, 5 x 10^{-1}]. The dropout rate is set to 0.1 for regularization purposes. The grid search technique is applied to the validation error using the cross-validation process described earlier. The sensitivity of the iTransformer to parameter tuning for the CALCE dataset is summarized in terms of RMSE validation error in Fig. 5. Similarly, tuning is performed for SC/MC-LSTM and SC/MC-Transformers for both the single and multi-channel approaches.

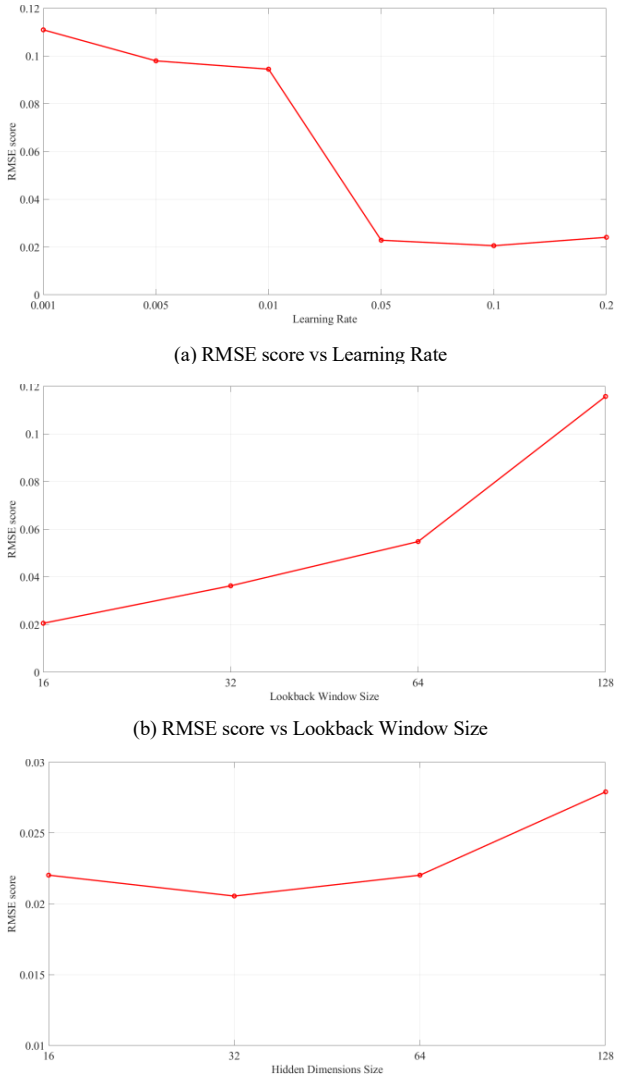

(a) RMSE score vs Learning Rate

(b) RMSE score vs Lookback Window Size

(c) RMSE score vs Hidden Dimension Size

Fig. 5. Validation error sensitivity to iTransformer parameters (CALCE)

B. NASA Battery Dataset

First, the discussed methods are applied to the battery sets 5, 6, 7, and 18. The RUL prediction results are presented in Fig. 6. Table I details the RMSE, MAE, and RE scores obtained for each battery after 3-fold cross-validation. It is observed that the multi-channel approaches incorporating the voltage, current, and temperature profiles perform significantly better than their single-channel counterparts. Using the MC approach considerably reduces the average RMSE score from 0.0751 to 0.0372 (50.47%) for LSTM and from 0.0551 to 0.0379 (31.22%) for Transformer. The iTransformer approach consistently

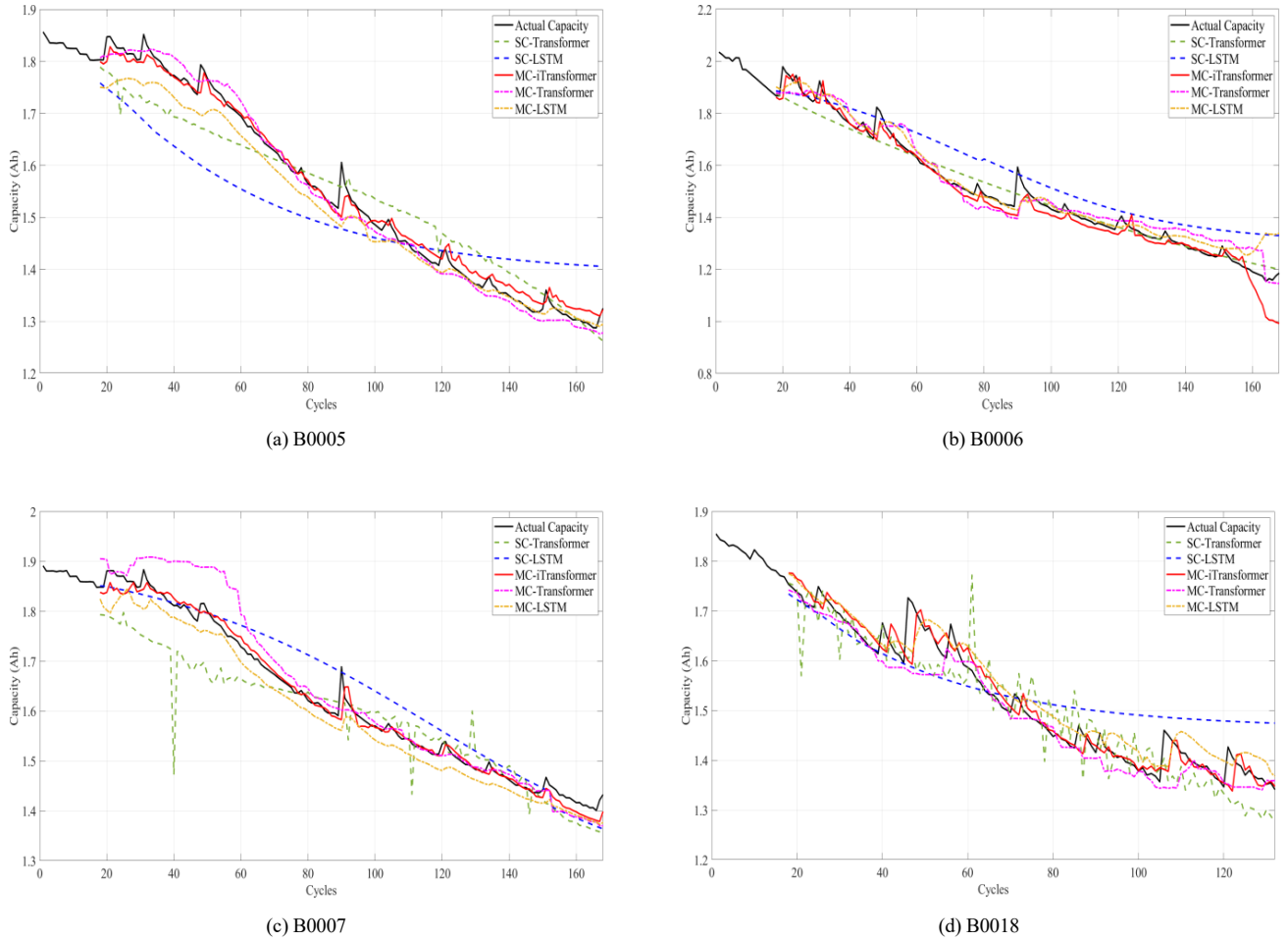

(a) B0005 (b) B0006

(c) B0007 (d) B0018

Fig. 6. Predicted Remaining Useful Life (RUL) for the NASA dataset

TABLE I. EVALUATION METRICS SUMMARY FOR NASA DATASET

Model	B0005			B0006			B0007			B00018		
	RMSE	*MAE*	*RE*	*RMSE*	*MAE*	*RE*	*RMSE*	*MAE*	*RE*	*RMSE*	*MAE*	*RE*
SC-Transformer	0.0554	0.0477	0.1129	0.0427	0.0312	0.0909	0.0658	0.0497	0.0893	0.0566	0.045	0.1311
SC-LSTM	0.0959	0.0842	0.3548	0.0863	0.0762	0.0826	0.047	0.0379	0.0774	0.0713	0.0595	0.082
MC-iTransformer	0.0185	0.0141	0.0242	0.0154	0.0283	0.0248	0.0243	0.0101	0.0536	0.0243	0.0213	0.0161
MC-Transformer	0.0227	0.0176	0.0564	0.0418	0.0325	0.0661	0.0438	0.0292	0.0714	0.0433	0.0285	0.0738
MC-LSTM	0.0371	0.0287	0.0484	0.0489	0.033	0.0825	0.0325	0.0288	0.0655	0.0302	0.0316	0.0574

outperforms all the SC/MC-LSTM and SC/MC-Transformer methods, achieving the lowest average RMSE score of 0.0206. For the individual battery sets, the MC-iTransformer has better accuracy than the best of the other four methods. From Fig. 5, it can be seen that battery #5 has the most regular degradation curve without appreciable regeneration. On the other hand, significant regeneration takes place for the other batteries, especially battery #18. Where the single channel approaches show significant deviation, the iTransformer demonstrates its real superiority in accurately capturing the capacity regeneration phenomenon. Even in the case of battery #18, where the degradation pattern is very different from the other three, the iTransformer is able to predict the multiple regeneration peaks throughout the cycle history.

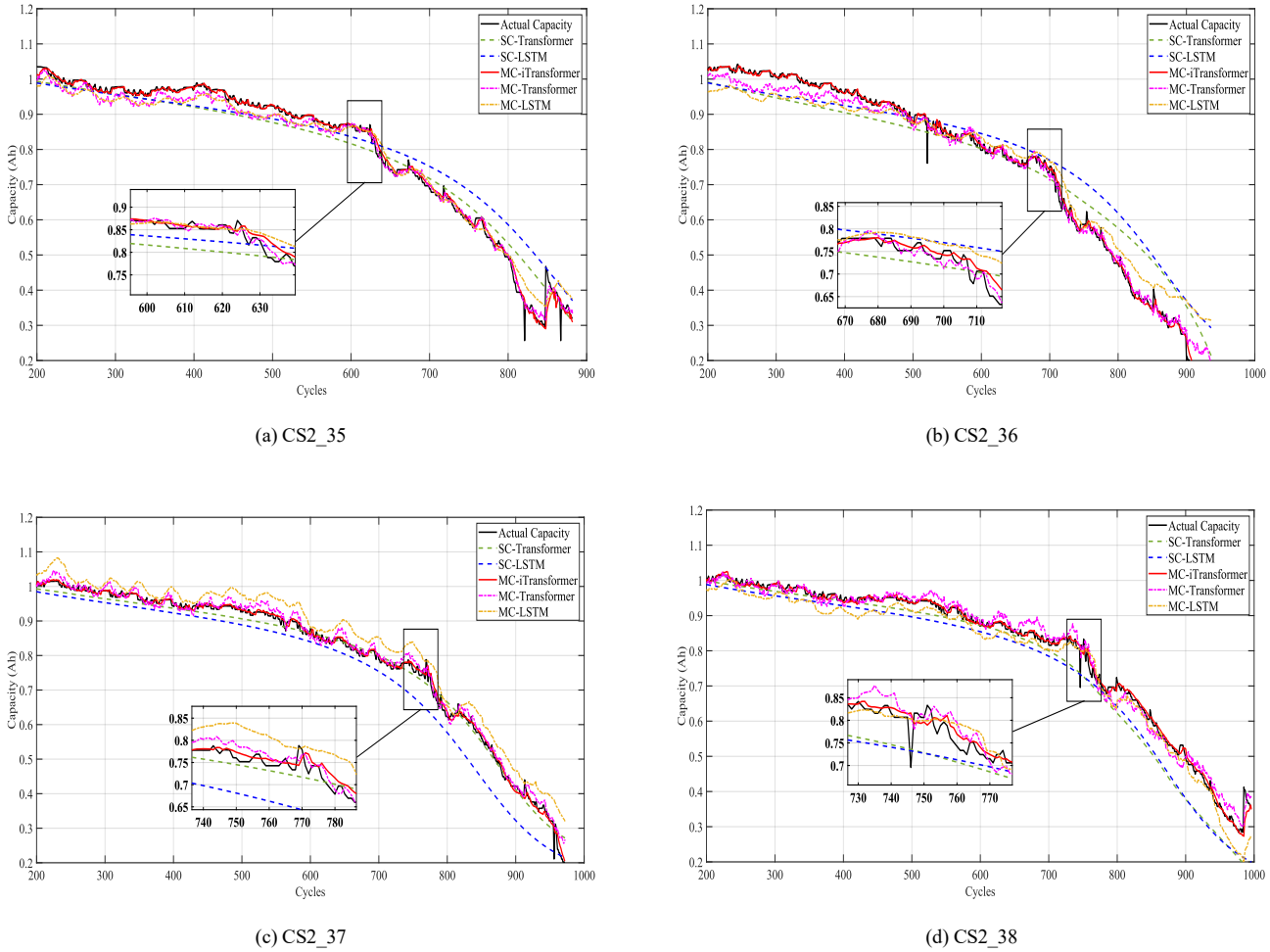

(a) CS2_35

(b) CS2_36

(c) CS2_37

(d) CS2_38

Fig. 7. Predicted Remaining Useful Life (RUL) for the CALCE dataset

TABLE II. EVALUATION METRICS SUMMARY FOR CALCE DATASET

Model	CS2_35			CS2_36			CS2_37			CS2_38		
	RMSE	*MAE*	*RE*	*RMSE*	*MAE*	*RE*	*RMSE*	*MAE*	*RE*	*RMSE*	*MAE*	*RE*
SC-Transformer	0.0331	0.0329	0.0139	0.0645	0.0530	0.0708	0.0219	0.0173	0.0532	0.0478	0.0378	0.0436
SC-LSTM	0.0564	0.0416	0.0588	0.0774	0.0606	0.0159	0.0557	0.0452	0.1104	0.0556	0.0441	0.0568
MC-iTransformer	0.0159	0.0079	0.0031	0.0160	0.0084	0.0087	0.0147	0.0081	0.0026	0.0386	0.0181	0.0026
MC-Transformer	0.0263	0.0183	0.0108	0.0414	0.0254	0.0144	0.0220	0.0144	0.0143	0.0303	0.0225	0.0119
MC-LSTM	0.0287	0.0234	0.0062	0.0617	0.0517	0.0159	0.0445	0.0384	0.0104	0.0712	0.0459	0.0132

C. CALCE Battery Dataset

First, the discussed methods are applied to the battery sets 35, 36, 37, and 38. The RUL prediction results are presented in Fig. 7. Table II details the RMSE, MAE, and RE scores obtained for each battery after 3-fold cross-validation. Similar to the NASA dataset, using the multi-channel approach, the average RMSE score drops from 0.0613 to 0.0515 (15.99%) for LSTM and from 0.0418 to 0.0300 (28.23%) for Transformer. The best accuracy is achieved by the iTransformer approach with mean RMSE & RE scores of 0.0213 and 0.0043, respectively. For the individual battery sets, the MC-iTransformer has better accuracy than the best of the other four methods. The key region of interest in these batteries is the range of 600-900 cycles where they reach the End of Life (EOL). In this region, the batteries demonstrate multiple instances of significant capacity regeneration. It is observed that the multi-channel methods are able to predict regeneration,

albeit with different accuracy. The MC-LSTM and MC-Transformer methods are comparable in performance in terms of their evaluation metrics as well as capacity regeneration prediction capability. The iTransformer, on the other hand, outperforms these methods at a higher learning rate, which also leads to lower training times.

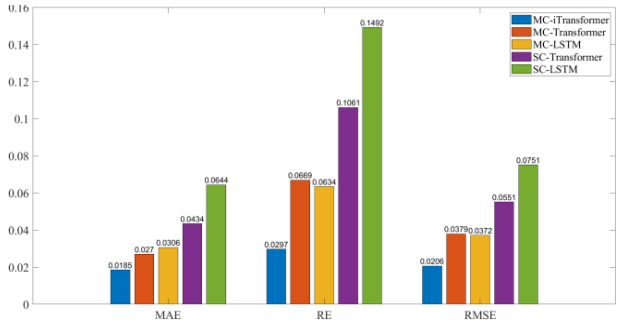

(a) NASA dataset

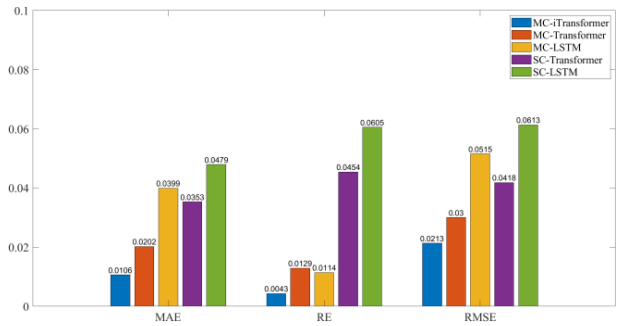

(b) CALCE dataset

Fig. 8. Average evaluation metrics for the NASA and CALCE dataset

VI. Conclusion & Future Work

In this paper, the recently introduced iTransformer architecture was investigated for predicting the Remaining Useful Life (RUL) of Li-ion batteries. It takes an inverted view of the capacity degradation series to capture multivariate correlations. Fig. 8 depicts the average evaluation metrics of all the five discussed approaches for the NASA and CALCE datasets. We demonstrated that the multi-channel approach lends itself better to RUL prediction than the single-channel approach. The iTransformer outperforms the vanilla transformer and the generally preferred LSTM method for both the NASA and CALCE battery datasets. Compared to the second-best techniques, it shows an improvement of 44.62% and 29% in the root mean square error (RMSE) for the NASA and CALCE datasets, respectively. In addition to having the least error, the iTransformer captures the battery regeneration phenomenon significantly better than the other methods. These results make it a promising technique for accurate RUL prediction. In the future, the effectiveness of the iTransformer should be explored on other battery chemistries such as NMC, NCA, and LFP on which other deep learning frameworks have shown good results. Further, in a typical driving scenario, the battery is only partially charged and discharged in narrow windows. The iTransformer can then be explored to extract the SOH information using partial charge/discharge cycles from a fast charge aging dataset as used in [22].

References

[1] J. Zhou, D. Liu, Y. Peng, and X. Peng, "Dynamic battery remaining useful life estimation: An on-line data-driven approach," *2012 IEEE International Instrumentation and Measurement Technology Conference Proceedings*, Graz, Austria, 2012, pp. 2196-2199, doi: 10.1109/I2MTC.2012.6229280.

[2] Seong Jin An, Jianlin Li, Claus Daniel, Debasish Mohanty, Shrikant Nagpure, David L. Wood, "The state of understanding of the lithium-ion-battery graphite solid electrolyte interphase (SEI) and its relationship to formation cycling", Carbon, Volume 105, 2016, Pages 52-76, ISSN 0008-6223, https://doi.org/10.1016/j.carbon.2016.04.008.

[3] Xiaosong Hu, Le Xu, Xianke Lin, Michael Pecht, "Battery Lifetime Prognostics," Joule, Volume 4, Issue 2, 2020, Pages 310-346, ISSN 2542-4351, https://doi.org/10.1016/j.joule.2019.11.018.

[4] Xin Li, Yan Ma, Jiajun Zhu, "An online dual filters RUL prediction method of lithium-ion battery based on unscented particle filter and least squares support vector machine," Measurement, Volume 184, 2021, 109935, ISSN 0263-2241.

[5] J. Yu, "State-of-health monitoring and prediction of lithium-ion battery using probabilistic indication and state-space model," IEEE Transactions on Instrumentation and Measurement 64 (11) (2015) 2937–2949.

[6] X. Su, S. Wang, M. Pecht, L. Zhao, Z. Ye, "Interacting multiple model particle filter for prognostics of lithium-ion batteries," Microelectronics Reliability 70 (2017) 59–69.

[7] Rui Wang, Mengmeng Zhu, Xiangwu Zhang, "Lifetime prediction and maintenance assessment of Lithium-ion batteries based on combined information of discharge voltage curves and capacity fade," Journal of Energy Storage, Volume 81, 2024, 110376, ISSN 2352-152X, https://doi.org/10.1016/j.est.2023.110376.

[8] C. Zhang, P. Lim, A. K. Qin, K. C. Tan, "Multiobjective deep belief networks ensemble for remaining useful life estimation in prognostics," IEEE transactions on neural networks and learning systems 28 (10) (2016) 2306–2318.

[9] Jungsoo Kim, Jungwook Yu, Minho Kim, Kwangrae Kim, Soohee Han, "Estimation of Li-ion Battery State of Health based on Multilayer Perceptron: as an EV Application," IFAC-PapersOnLine, Volume 51, Issue 28, 2018, Pages 392-397, ISSN 2405-8963, https://doi.org/10.1016/j.ifacol.2018.11.734.

[10] B. Chinomona, C. Chung, L. -K. Chang, W. -C. Su and M. -C. Tsai, "Long Short-Term Memory Approach to Estimate Battery Remaining Useful Life Using Partial Data," in IEEE Access, vol. 8, pp. 165419-165431, 2020, doi: 10.1109/ACCESS.2020.3022505.

[11] Y. Song, L. Li, Y. Peng, and D. Liu, "Lithium-Ion Battery Remaining Useful Life Prediction Based on GRU-RNN," 2018 12th International Conference on Reliability, Maintainability, and Safety (ICRMS), Shanghai, China, 2018, pp. 317-322, doi: 10.1109/ICRMS.2018.00067.

[12] A. Vaswani et al., N. Shazeer, N. Parmar, J. Uszkoreit, L. Jones, A. N. Gomez, L. Kaiser, and I. Polosukhin, "Attention is all you need," in Proc. Adv. Neural Inf. Process. Syst., 2017, pp. 5998–6008.

[13] Yong Liu et al., " iTransformer: Inverted Transformers Are Effective for Time Series Forecasting," The Twelfth International Conference on Learning Representations, 2024.

[14] C. Wang, N. Lu, S. Wang, Y. Cheng, and B. Jiang, "Dynamic long short term memory neural-network based indirect remaining-useful-life prognosis for satellite lithium-ion battery," Appl. Sci., vol. 8, no. 11, p. 2078, Oct. 2018.

[15] K. Goebel, B. Saha, A. Saxena, J. R. Celaya, and J. P. Christophersen, ''Prognostics in battery health management,'' IEEE Instrum. Meas. Mag., vol. 11, no. 4, pp. 33–40, Aug. 2008.

[16] B. Saha and K. Goebel, Battery Data Set NASA Ames Prognostics Data Repository, 2007.

[17] Y. Xing, E. W. M. Ma, K.-L. Tsui, and M. Pecht, "An ensemble model for predicting the remaining useful performance of lithium-ion batteries," Microelectron. Rel., vol. 53, pp. 811–820, Jun. 2013.

[18] Chen Fei, October 13, 2022, "Lithium-ion battery data set", IEEE Dataport, doi: https://dx.doi.org/10.21227/fh1g-8k11.

[19] Zhang, Han, et al. "Harnessing Intra-and Inter-Cell Differences: A Comprehensive Approach to Precise Battery Lifespan Estimations across Conditions." arXiv preprint arXiv:2310.05052 (2023).

[20] Y. Choi, S. Ryu, K. Park, and H. Kim, ‘‘Machine learning-based lithium-ion battery capacity estimation exploiting multi-channel charging profiles,’’ IEEE Access, vol. 7, pp. 75143–75152, 2019.

[21] A. Jain, K. Nandakumar, and A. Ross, ‘‘Score normalization in multimodal biometric systems,’’ Pattern Recognit., vol. 38, no. 12, pp. 2270–2285, Dec. 2005.

[22] J. Chen et al., "A Convolutional Neural Network for Estimation of Lithium-Ion Battery State-of-Health during Constant Current Operation," 2023 IEEE Transportation Electrification Conference & Expo (ITEC), Detroit, MI, USA, 2023, pp. 1-6.